Engineered Science
DOI: https://dx.doi.org/10.30919/es1380

The Role of Copper Incorporation in Improving the Electrical Insulation Properties of Microarc Oxidation Coatings on Aluminum Alloys

Lina Shehadeh,[1,*] Khairudin Mohamed,[1] Ubeidulla Al-Qawabeha[2] and Basim Abu-Jdayil[3]

Abstract

This study explores the effect of varying copper content on the electrical conductivity of microarc oxidation (MAO) coating films applied to aluminum alloy substrates. The experimental setup involved preparing (Al–X%Cu) alloys and subjecting them to MAO treatment. The MAO coatings were analyzed via scanning electron microscopy (SEM) and X-ray diffraction (XRD) to examine their chemical composition, surface morphologies, and phase structures. Results revealed that increasing Cu content up to 3 wt.% in Al alloys led to the formation of α-Al_2O_3 and ɣ-Al_2O_3 phases, which serve as electrical insulators, thereby reducing the electrical conductivity and enhancing the dielectric properties of the coating layer. Despite this, electrical conductivity measurements of MAO coatings on (Al-6% Cu) and (Al-9% Cu) alloys yielded values of 4.17 and 5.27 S/m, respectively, because of the presence of CuO phases, which improved electrical conductivity in these alloys. Thus, the findings indicated that higher Cu content increases electrical conductivity of coatings and makes it not fully insulated, despite that the MAO coating films have insulating properties as indicated in previous studies.

Keywords: Alumina; Coating; Electrical conductivity; Microarc oxidation process.
Received: 18 October 2024; Revised: 08 November 2024; Accepted: 02 December 2024.
Article type: Research article.

1. Introduction

In the field of electronics and materials, the research and fabrication of innovative dielectric materials (insulating materials) for diverse applications has been actively focused on.[1–4] Alumina ceramics are commonly employed as insulators in numerous high-voltage devices due to their notable attributes, including high dielectric breakdown strength, minimal electrical losses, elevated hardness, and excellent thermal stability.[5–9] Among various forms of aluminum oxide, α-Al_2O_3 or corundum is particularly important because of its stable thermodynamic properties. α-alumina is employed in diverse applications as electronic components, serving as electrical insulators, light-emitting displays, cutting tools, lasers, gas sensors, and spark plugs.[10–12]

Al alloys are extensively used across diverse industries, including aerospace, automotive, and shipbuilding because of their exceptional mechanical characteristics, impressive strength-to-weight ratio, and cost-effective manufacturing processes.[13] Various alloying elements, such as Cu, Zn, Mg, Si, Mn, and Li, can be incorporated into these alloys, yielding different series of Al alloys.[14]

Al–Cu is the most common cast Al alloy system. Cu addition increases the strength and hardness of Al at all temperatures and during all heat treatment processes, thereby improving the machinability of alloys. However, Cu tends to precipitate at grain boundaries, increasing the susceptibility of Al alloys to various types of corrosion.[15,16] The surface properties of Al alloys can be altered by various methods. In particular, surface modification techniques such as the use of superhydrophobic surfaces, anodic oxidation, and microarc oxidation (MAO) have been extensively investigated to improve the corrosion resistance of Al in corrosive environments. Most coatings are mechanically bonded with the substrate to improve its corrosion resistance to a certain

[1] *School of Mechanical Engineering, Engineering Campus, Universiti Sains Malaysia, Nibong Tebal, Penang, 14300, Malaysia*
[2] *Faculty of Mechanical engineering, Tafila Technical university, Tafila, 66110, Jordan*
[3] *Chemical & Petroleum Engineering Department, United Arab Emirates University, PO Box 15551, United Arab Emirates*
[#] *These authors contributed to this work equally.*
**Email:* ileena82@yahoo.com (L. Shehadeh)

extent. MAO differs in this respect from other methods because it forms excellent metallurgical bonds between the substrate and coating.[17,18] The MAO process is commonly employed to enhance electrical barriers in Al, creating a strong adherent coating by converting the Al substrate into γ-$A1_2O_3$ and α-$A1_2O_3$ alumina.[19–22] MAO process transforms a metal specimen surface into a ceramic coating through a series of electrical sparks.

Fig. 1 shows the MAO process procedure. As the inside of a stainless-steel tank is filled with a specific electrolyte, the metal specimen as anode is zapped with a high voltage supply. This voltage creates a continuous stream of tiny sparks between the metal specimen and cathode electrode. After several minutes to tens of minutes of this sparking, a dense uniform layer of oxide is formed on the surface of the metal specimen. This oxide layer has varied porosity and specific chemical composition depending on the metal specimen and electrolyte used.[23–26]

Regardless of whether alternating current (AC) or direct current (DC) power is used, the basic principles of MAO coating formation remain the same. As the applied voltage increases, a permeable insulating layer begins to form, characterized by a columnar structure and the production of numerous gas bubbles, as illustrated in Fig. 2. When the voltage reaches the breakdown point in certain weak spots within the insulating layer, dielectric breakdown and spark discharge occur. This leads to the appearance of fine white sparks evenly distributed on the sample surface. As the number of sparks decreases, small uniform micropores are created. During the MAO process, the sparks gradually change color, starting from white and transitioning to yellow, eventually becoming orange red. The shift from yellow to orange-red in the microarc stage is associated with a rapid coating growth rate. As both the voltage and coating thickness increase, the number of sparks reduces, but their intensity grows, resulting in rougher surface morphologies. With further increasing the voltage, a porous and loosely structured region of the MAO coating is formed.[27,28]

Several factors influence the quality of the MAO layer coating, including the composition of the substrate, concentration and temperature of the electrolyte, treatment process duration, and electrical parameters of the MAO process.[29–31] While numerous studies have focused on improving the properties of MAO coatings by refining the electrolyte pairings and electrical parameters, the effects of alloying elements on the dielectric properties of aluminum have not been thoroughly examined.

To the best of our knowledge, only a few existing articles discuss the influence of various elements (*i.e.*, Li, Mg, Fe and Si) on the characteristics of resulting MAO coatings for commercially available aluminum alloys.[32–34] Furthermore, limited studies have specifically focused on the effects of individual alloying elements within the substrate on the dielectric properties of substrates. For example, Zhu *et al.* investigated the effect of Cu concentration on the corrosion resistance and microstructure of MAO coatings.[35] The findings revealed that Cu in the substrate alloy enhanced the transformation process and intensity of microdischarges, leading to the formation of cracks and pores in the MAO coatings because of oxygen release, which is due to the dissolution of copper oxide (CuO) and oxidation of O^{2-}. Concurrently, the average porosity of MAO coatings substantially increased with increasing the copper content, a critical factor contributing to the reduced corrosion resistance of MAO films. Dai *et al.* conducted research involving the fabrication of MAO coating films on Al–Cu alloys with varying oxidation durations and observed that the thickness, surface roughness, cracks, porosity, and α-Al_2O_3 content of MAO coatings increased in the Al–4.5%Cu alloy.[36]

Many previous studies have investigated the effects of substrate composition on the mechanical properties of the coatings. However, information on the role of elements in

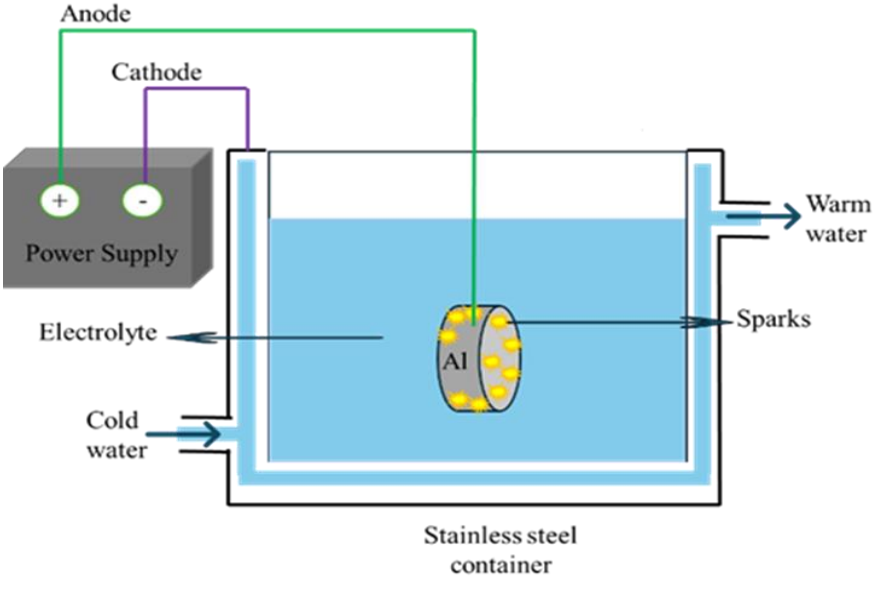

Fig. 1: Schematic of the MAO system showing the equipment arrangement.

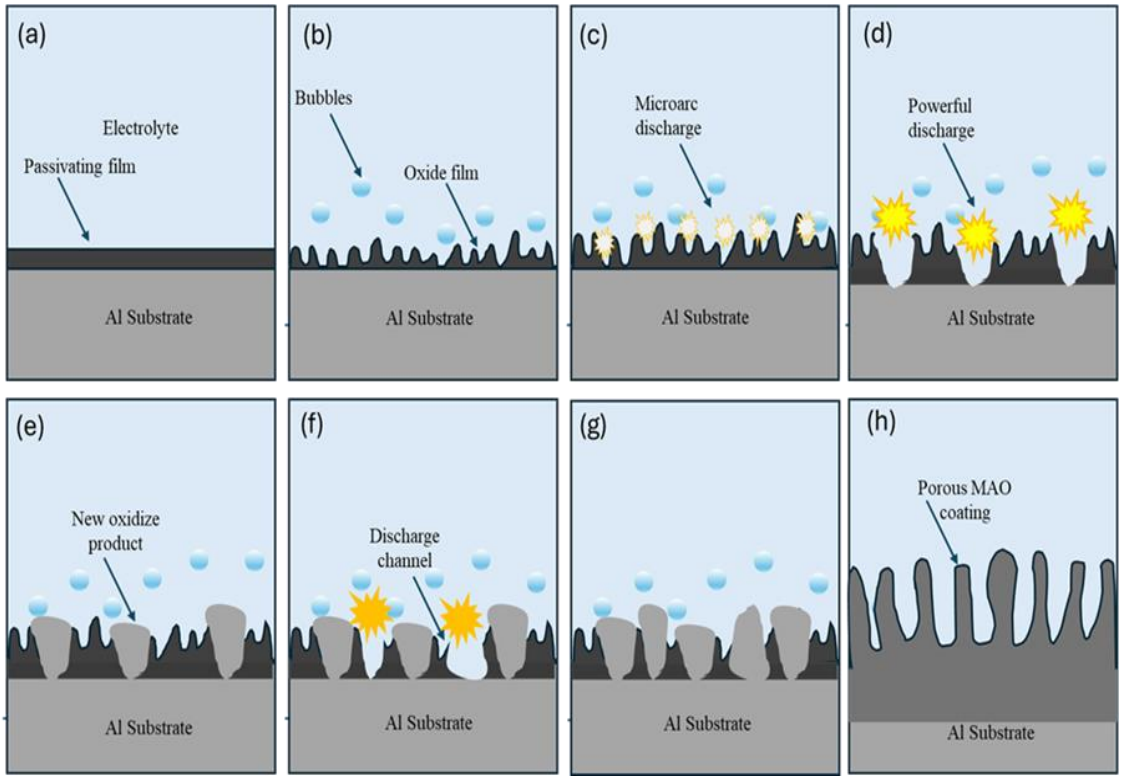

Fig. 2: Schematic of the growth mechanism of MAO coating: (a) passivating film before applying high voltage, (b) initial formation of an oxide film, (c) initiation of microarc discharges, (d) occurrence of more powerful discharges, (e) deposition of new oxidized products in the discharge channels, (f) formation of discharge channels as a result of continuous microarc discharges, (g) further growth of the oxide, and (h) final stage showing a fully developed porous MAO coating.

2. Experimental methods

2.1 Materials and pretreatment

For this investigation, cylindrically shaped Al–X%Cu alloy specimens with dimensions of 15 mm in diameter and 7 mm in thickness prepared at Al-Zaytoonah University were utilized as the base material for MAO experiments. The chemical composition of the prepared Al alloys is listed in Table 1. Prior to MAO process, all specimens underwent a sequential grinding process using abrasive papers with decreasing grit sizes (from 180 to 1200) to eliminate surface oxides. Subsequently, the specimens underwent polishing using a polishing machine to eliminate imperfections. Finally, all specimens were degreased with acetone, cleaned in ethanol for 12 min, rinsed with distilled water, and finally dried in ambient air.

Table 1: Chemical composition of Al–Cu alloys (wt.%).

Code	Alloy	Al	Cu
A	Al	99.99	0.0
B	Al-1%Cu	98.92	1.07
C	Al-3%Cu	96.94	3.05
D	Al-6%Cu	93.93	6.06
E	Al-9%Cu	90.91	9.08

2.2 MAO coating process setup

MAO coatings were uniformly applied to all specimen surfaces using a consistent pulse current density of 1 A/cm² of coating process for 60 min. The apparatus utilized for the process was equipped at Al-Zaytoonah University, Amman, Jordan with a cooling system by circulating cooling water, which was designed to regulate the electrolyte temperature. This study utilizes an aluminum alloy specimen as the anode electrode. The cathode electrode is a stainless-steel electrolytic bath, as shown in Fig. 3. The MAO coating is formed in an alkaline-based electrolytic bath containing 2 g/L potassium hydroxide (KOH) and 12 g/L sodium silicate (Na_2SiO_3). The MAO process employs alternating current (AC) mode throughout most of the procedure, switching to constant voltage mode once a voltage of 240 V is achieved. Following the process, the specimens are cleaned with deionized water and dried.

2.3 Chemical composition, surface morphology, and phase structure of MAO coating films

The surface morphologies and chemical composition of the MAO-coated film specimens were analyzed using scanning electron microscopy (SEM) and energy dispersive X-ray (EDX) analyses (JEOL JSM 6390A). EDX analysis was performed randomly on the film surface, and the final composition was derived from an average of seven parallel point analyses. Furthermore, X-ray diffraction (XRD) was employed to investigate the phase structure of MAO films.

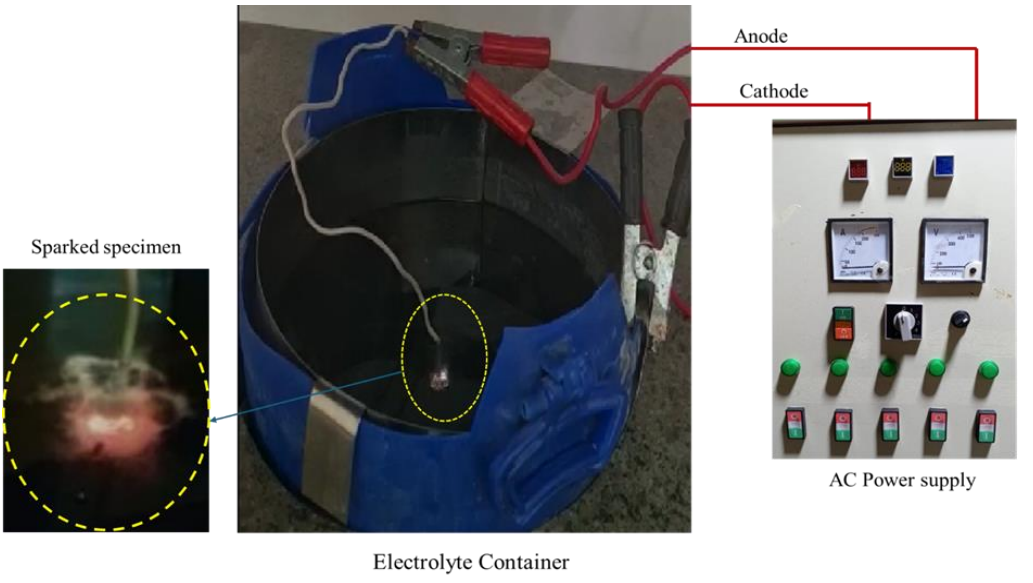

Fig. 3: Experimental setup of the MAO process.

2.4 Electrical conductivity of the MAO films

The I–V characteristics of ceramic varistors were assessed by using a source measurement unit (Keithley 236). Using simultaneous current measurements, the resistances of these ceramic varistors were determined by analyzing the I–V slopes obtained through cyclic potential cycling from −2.0 to +2.0 V at a sweep rate of 0.01 V/s. The material's resistivity (σ) was calculated by evaluating the physical and resistance dimensions of the material utilizing equation (1):

$$\sigma = L/RA \quad (1)$$

where R represents specimen resistance, A denotes surface area, and L is specimen thickness.

3. Results and discussion

3.1 Chemical composition, surface morphology, and phase structure of MAO films

Fig. 4 presents five micrographs labeled A through E, which are the SEM images showing the surface morphology of MAO coatings applied to five distinct specimens. Each image highlights a small area marked by a cyan square, within which the elemental composition is analyzed. This area is subjected to EDX analysis, providing detailed information on the mass

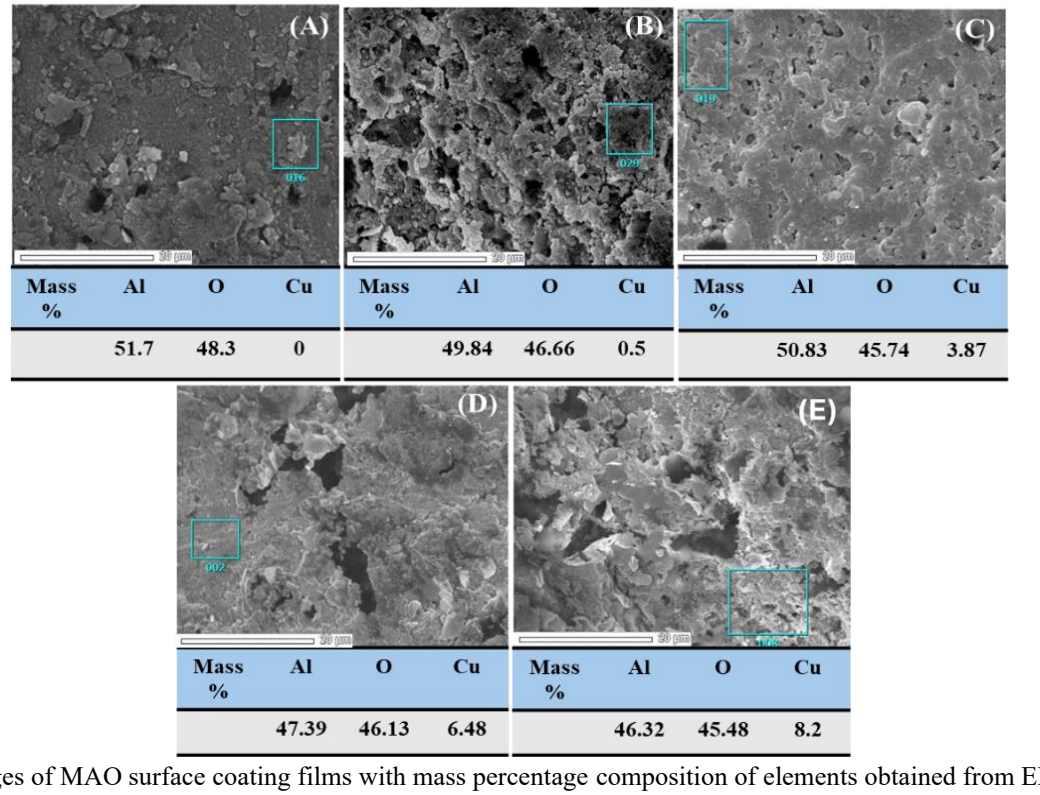

Mass %	Al	O	Cu
(A)	51.7	48.3	0
(B)	49.84	46.66	0.5
(C)	50.83	45.74	3.87
(D)	47.39	46.13	6.48
(E)	46.32	45.48	8.2

Fig. 4: SEM images of MAO surface coating films with mass percentage composition of elements obtained from EDX analysis of five specimens (A, B, C, D, and E).

percentages of Al, O, and Cu in the coatings.

Fig. 4A represents the surface composition of a specimen with pure Al on the coating, with no copper content detected in the film. Figs. 4B to 4E show the compositions of Al alloys with varying amounts of Cu incorporated into the MAO coating. These figures demonstrate an increase in Cu content as the alloy composition changes. The analysis reveals that the percentage of copper in the coating increases progressively from B to E, with the highest concentration of Cu observed in specimen E.

The EDX analysis confirms that the incorporation of Cu in the coating film is primarily in the form of (CuO), as identified by Gao team,[37] the MAO coating films contain Cu primarily in the form of copper (II) oxide (CuO). This suggests that Cu in the alloy undergoes oxidation during the MAO process, contributing to the overall composition of the surface film.

These findings align closely with the XRD results, as depicted in Fig. 5, which presents the XRD patterns of the MAO films. The XRD analysis provides additional confirmation of the elemental compositions detected by EDX, reinforcing the identification of the phases present in the coatings. The diffraction peaks reveal that all MAO coatings consist of both γ-Al_2O_3 (gamma-alumina) and α-Al_2O_3 (alpha-alumina), along with distinct peaks attributed to the Al alloy substrate.

The presence of α-Al_2O_3 is particularly notable due to its highly stable nature. This phase is characterized by extreme hardness and a high melting point of around 2050 °C, making it an ideal protective coating. The stability and toughness of α-Al_2O_3 contribute to the overall durability of the MAO coatings, especially in high-temperature or corrosive environments. In contrast, γ-Al_2O_3 is classified as a metastable phase, which means that it can convert into α-Al_2O_3 over time when exposed to elevated temperatures, typically between 800 °C and 1200 °C, as reported by Wei *et al*.[38]

The XRD analysis for specimens C, D, and E reveals distinct peaks corresponding to CuO in addition to the α-Al_2O_3 and γ-Al_2O_3 phases. These peaks confirm the presence of copper oxide in the MAO coatings of the samples with higher copper content. The appearance of CuO is consistent with the EDX results, reinforcing the conclusion that copper in the aluminum alloys undergoes oxidation during the MAO process, forming a copper oxide layer. This finding aligns with the observations reported by Rokosz *et al.* (2016), who documented similar CuO peaks in their study of MAO coatings on copper-containing alloys.[26]

It is important to note that in the XRD patterns of pure aluminum (specimen A) and alloys with a low Cu content—Al-1%Cu (specimen B) and Al-3%Cu (specimen C), the CuO peaks are notably absent. This absence is due to the relatively low percentage of Cu in these substrates. In alloys with minimal Cu content, the formation of significant amounts of CuO during the MAO process is limited, which explains why no CuO peaks are detected in the XRD patterns of these samples. The limited Cu content in these specimens likely leads to a lower degree of oxidation and incorporation of CuO into the MAO coating.

The presence of CuO peaks in the XRD patterns for specimens with a higher Cu content (D and E) also suggests that the concentration of Cu in the alloy directly influences the phase composition of the MAO coatings. As the Cu percentage increases, the probability of Cu oxidation and CuO formation also increases, resulting in stronger CuO peaks in the XRD analysis. This correlation between copper content and oxide formation is crucial for understanding the electrical and corrosion-resistant properties of the coatings, as CuO plays a significant role in enhancing these characteristics.

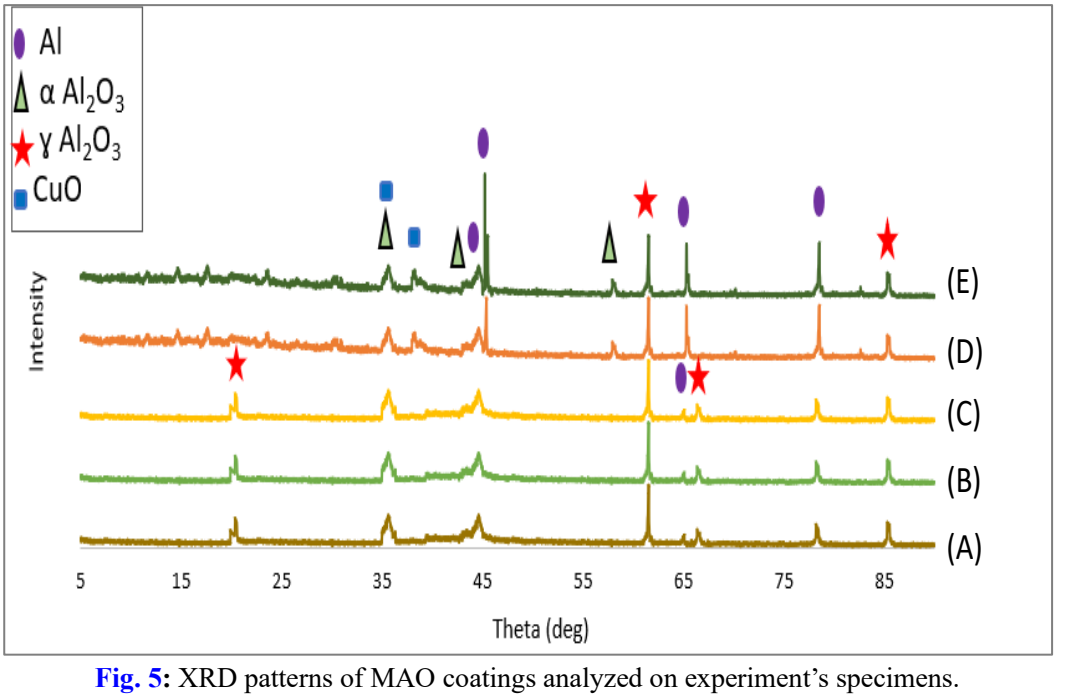

Fig. 5: XRD patterns of MAO coatings analyzed on experiment's specimens.

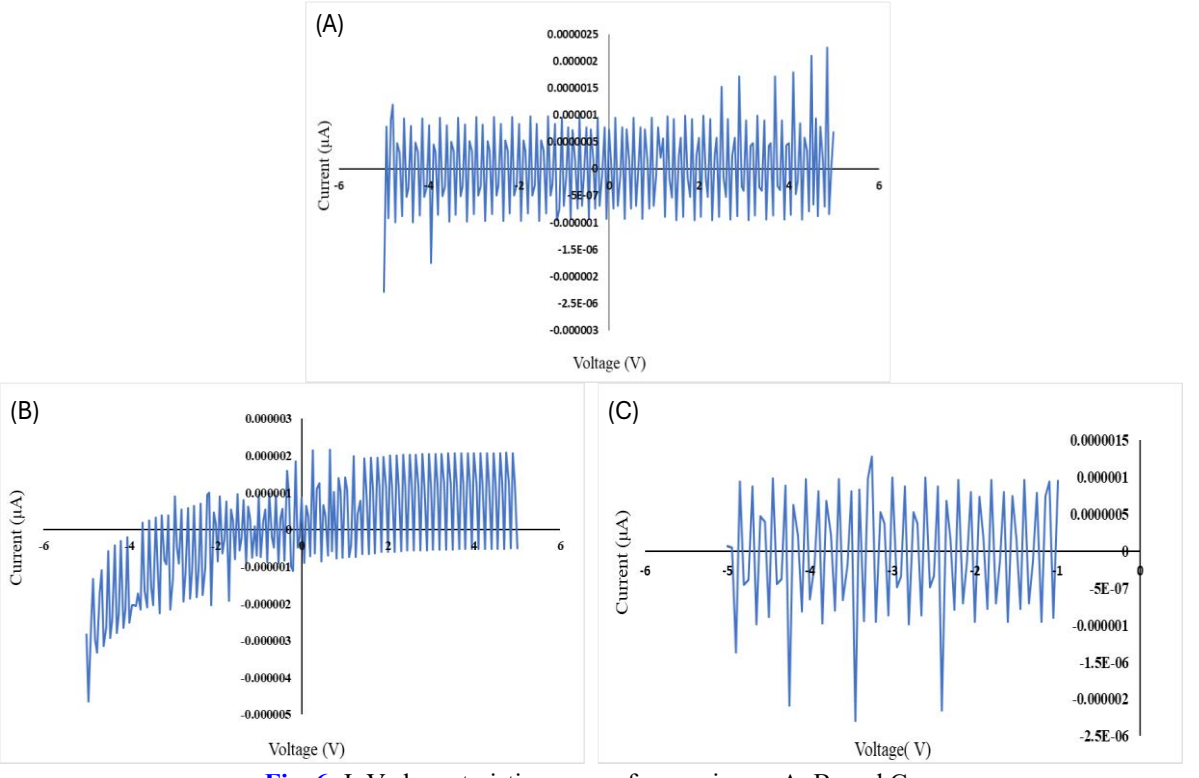

Fig. 6: I–V characteristics curves for specimens A, B, and C.

3.2 Electrical conductivity

Fig. 6 presents the current-voltage (I–V) curves for specimens A, B, and C, which highlight their electrical insulating properties. These curves demonstrate that the materials exhibit minimal or no current leakage under low applied voltages, indicating a strong insulation behavior. This is especially evident at the lower end of the voltage range, where the current remains close to zero, a characteristic typically expected in materials with a high electrical resistivity.

The insulating properties observed in the I–V curves are primarily attributed to the MAO coating formed on the Al. The formed coating is a ceramic oxide layer that consists predominantly of α-Al_2O_3 and γ-Al_2O_3 phases. Both alumina phases are known for their excellent insulating characteristics, which stem from their ceramic nature.

These alumina phases are effective electrical insulators due to their high bandgap, which means that the material lacks free electrons or mobile charge carriers necessary for conducting

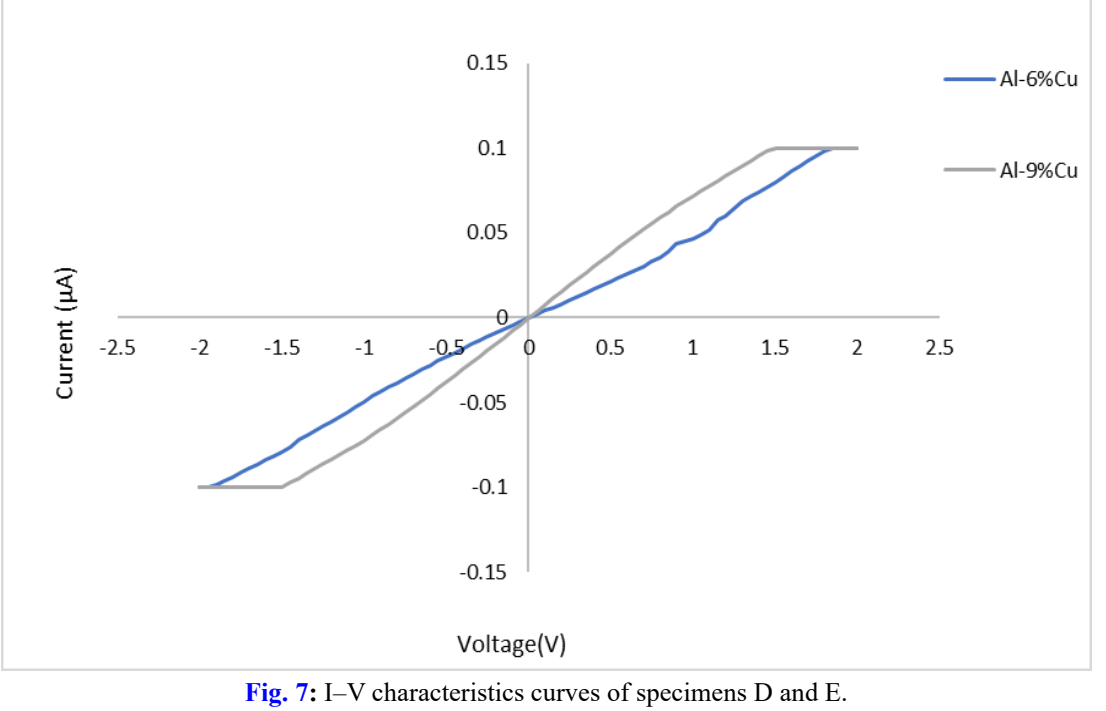

Fig. 7: I–V characteristics curves of specimens D and E.

current. The absence of such charge carriers in these ceramic materials explains the minimal current flow observed in the I–V curves at low voltages.[39]

Fig. 7 shows an evident linear response of I-V characteristics curve for Al 6%Cu and Al 9%Cu alloys. The gradient of the curve provides the conductance value, which is used to calculate the electrical conductivity of the specimens. The electrical conductivity of Al-6%Cu and Al-9%Cu are 4.17 and 5.27 S/m, respectively. Notably, a higher electrical conductivity value is observed at an elevated Cu content, indicating the influence of CuO electrons on the electrical conductivity of alloys. This is attributed to the presence of metallic Cu inclusions within CuO, positively contributing to conductivity.[40] The existing mobile charge carriers (electrons or ions) can move without restrictions within the material and determine the conductivity of the material.[41] In the case of pure α-Al_2O_3, free charge carriers are not available, hence, its conductivity is zero. However, when CuO is combined with α-Al_2O_3, Cu^{2+} is introduced into the material, and acts as charge carriers, thereby enhancing the conductivity of the material.[42,43] Table 2 shows the summary of the electrical conductivity results.

Table 2: Summary of the electrical conductivity results.

Specimen code	Copper content (%)	Electrical conductivity (S/m)
A	0	Insulating
B	1	Insulating
C	3	Insulating
D	6	4.17
E	9	5.27

4. Conclusion

This study demonstrated the influence of varying Cu content in Al alloys on the electrical insulation and conductivity properties of MAO coatings. The results indicate that increasing Cu content in Al-Cu alloys contributes to a higher presence of copper oxide (CuO) within the MAO coating layer. While MAO coatings generally enhance electrical insulation due to alumina phases (i.e., α-Al_2O_3 and γ-Al_2O_3), higher copper concentrations lead to increased conductivity, as observed with Al-6%Cu and Al-9%Cu alloys. These findings underscore the dual effect of copper incorporation: improving certain conductive properties while potentially limiting the insulating capability of the MAO coating, which could be optimized based on the intended application. Future work could further investigate the balance between conductivity and insulation in Al-Cu alloys to develop coatings with tailored electrical properties for specific engineering applications.

Conflict of Interest

There is no conflict of interest.

Supporting Information

Not applicable.

References

[1] H. P. Palani Velayuda Shanmugasundram, E. Jayamani, K. H. Soon, A comprehensive review on dielectric composites: Classification of dielectric composites, *Renewable and Sustainable Energy Reviews*, 2022, **157**, 112075, doi: 10.1016/j.rser.2022.112075.

[2] Y. Feng, Q. Wu, Q. Deng, C. Peng, J. Hu, Z. Xu, High dielectric and breakdown properties obtained in a PVDF based nanocomposite with sandwich structure at high temperature via all-2D design, *Journal of Materials Chemistry C*, 2019, **7**, 6744-6751, doi: 10.1039/C9TC01378D.

[3] C. Gabriel, Dielectric properties of biological materials, 2018.

[4] K. R. Foster, H. P. Schwan, Dielectric properties of tissues, 2019.

[5] W. Xu, P. Li, C. Zhang, M. Zhong, Y. Shao, Z. Li, D. Liu, Z. Zhang, Dielectric breakdown strength of alumina ceramics reinforced by fractal dendritic $Ca_9Al(PO_4)_7$ as the second crystalline phase, *Journal of Alloys and Compounds*, 2020, **832**, 154811, doi: 10.1016/j.jallcom.2020.154811.

[6] M. Touzin, D. Goeuriot, C. Guerret-Piécourt, D. Juvé, H. J. Fitting, Alumina based ceramics for high-voltage insulation, *Journal of the European Ceramic Society*, 2010, **30**, 805-817, doi: 10.1016/j.jeurceramsoc.2009.09.025.

[7] D. Malec, V. Bley, F. Talbi, F. Lalam, Contribution to the understanding of the relationship between mechanical and dielectric strengths of Alumina, *Journal of the European Ceramic Society*, 2010, **30**, 3117-3123, doi: 10.1016/j.jeurceramsoc.2010.07.024.

[8] C. Qian, K. Hu, Z. Shen, Q. Wang, P. Li, Z. Lu, Effect of sintering aids on mechanical properties and microstructure of alumina ceramic *via* stereolithography, *Ceramics International*, 2023, **49**, 17506-17523, doi: 10.1016/j.ceramint.2023.02.118.

[9] R. Danzer, On the relationship between ceramic strength and the requirements for mechanical design, *Journal of the European Ceramic Society*, 2014, **34**, 3435-3460, doi: 10.1016/j.jeurceramsoc.2014.04.026.

[10] J. Shah, S. K. Gupta, Y. Sonvane, K. Adhikari, Computational study of electronic and optical properties of p-group atomic adsorption on α-Al_2O_3 (0001), *Computational and Theoretical Chemistry*, 2019, **1155**, 101-108, doi: 10.1016/j.comptc.2019.03.026.

[11] T. yan, X. Guo, X. Zhang, Z. Wang, J. Shi, Low temperature synthesis of nano alpha-alumina powder by two-step hydrolysis, *Materials Research Bulletin*, 2016, **73**, 21-28, doi: 10.1016/j.materresbull.2015.08.021.

[12] A. Eftekhari, B. Movahedi, G. Dini, M. Milani, Fabrication and microstructural characterization of the novel optical ceramic consisting of α-Al_2O_3@amorphous alumina nanocomposite core/shell structure, *Journal of the European Ceramic Society*, 2018, **38**, 3297-3304, doi: 10.1016/j.jeurceramsoc.2018.02.038.

[13] T. Arunkumar, T. Selvakumaran, R. Subbiah, K. Ramachandran, S. Manickam, Development of high-performance aluminium 6061/SiC nanocomposites by ultrasonic aided rheo-squeeze casting method, *Ultrasonics Sonochemistry*, 2021, **76**, 105631, doi: 10.1016/j.ultsonch.2021.105631.

[14] T. Shetty, J. Pai, N. Naik, A. V. Samrot, P. Bhat, S. S A, Protection of magnesium AZ31B alloy in a hydrochloric acid medium using gelatin and optimizing the results through response surface methodology, *ES Materials & Manufacturing*, 2023, **22**, 1066, doi: 10.30919/esmm1066.
[15] L. Mulky, P. Rao, Effect of operational parameters on fouling of 6061 aluminum alloy under dynamic conditions, *ES Materials & Manufacturing*, 2023, **21**, 893, doi: 10.30919/esmm893.
[16] J. Hindi, A. Murthy A, K. Muralishwara, K. Kasipandian, G. B M, N. Naik, Tribological characterization of precipitation hardened 7075 aluminium alloy composites reinforced with cast iron particle, *ES Materials & Manufacturing*, 2023, **22**, 1034, doi: 10.30919/esmm1034.
[17] Q. Zhu, B. Zhang, X. Zhao, B. Wang, Binary additives enhance micro arc oxidation coating on 6061Al alloy with improved anti-corrosion property, *Coatings*, 2020, **10**, 128, doi: 10.3390/coatings10020128.
[18] Z. Lin, T. Wang, X. Yu, X. Sun, H. Yang, Functionalization treatment of micro-arc oxidation coatings on magnesium alloys: a review, *Journal of Alloys and Compounds*, 2021, **879**, 160453, doi: 10.1016/j.jallcom.2021.160453.
[19] L. Xia, J. Han, J. P. Domblesky, Z. Yang, W. Li, Investigation of the scanning microarc oxidation process, *Advances in Materials Science and Engineering*, 2017, **2017**, 2416821, doi: 10.1155/2017/2416821.
[20] A. A. Snezhko, T. V. Strekaleva, N. V. Zakharova, E. K. Vasilyeva, E. A. Karelina, The influence of the chemical composition of aluminum on the quality of coatings formed using microarc oxidation, *Journal of Physics*: *Conference Series*, 2022, **2373**, 072045, doi: 10.1088/1742-6596/2373/7/072045.
[21] V. V. Subbotina, O. V. Sobol, V. V. Belozerov, V. V. Schneider, U. F. Al-Qawabeha, T. A. Tabaza, S. M. Al-Qawabah, Increase of the α-Al_2O_3 phase content in MAO-coating by optimizing the composition of oxidated aluminum alloy, *Functional Materials*, 2019, **26**, 752-758, doi: 10.15407/fm26.04.752.
[22] N. Xiang, R. Song, J. Zhao, H. Li, C. Wang, Z. Wang, Microstructure and mechanical properties of ceramic coatings formed on 6063 aluminium alloy by micro-arc oxidation, *Transactions of Nonferrous Metals Society of China*, 2015, **25**, 3323-3328, doi: 10.1016/S1003-6326(15)63988-7.
[23] F. Simchen, M. Sieber, A. Kopp, T. Lampke, Introduction to plasma electrolytic oxidation: an overview of the process and applications, *Coatings*, 2020, **10**, 628, doi: 10.3390/coatings10070628.
[24] A. Sobolev, I. Wolicki, A. Kossenko, M. Zinigrad, K. Borodianskiy, Coating formation on Ti-6Al-4V alloy by micro arc oxidation in molten salt, *Materials*, 2018, **11**, 1611, doi: 10.3390/ma11091611.
[25] Y. Dong, Z. Liu, G. Ma, The research progress on micro-arc oxidation of aluminum alloy, *IOP Conference Series*: *Materials Science and Engineering*, 2020, **729**, 012055, doi: 10.1088/1757-899x/729/1/012055.
[26] K. Rokosz, T. Hryniewicz, Ł. Dudek, Phosphate porous coatings enriched with selected elements *via* PEO treatment on titanium and its alloys: a review, *Materials*, 2020, **13**, 2468, doi: 10.3390/ma13112468.
[27] T. Shetty, J. Pai, N. Naik, A. V. Samrot, P. Bhat, S. S A, Protection of magnesium AZ31B alloy in a hydrochloric acid medium using gelatin and optimizing the results through response surface methodology, *ES Materials & Manufacturing*, 2023, **22**, 1066, doi: 10.30919/esmm1066.
[28] L. Mulky, P. Rao, Effect of operational parameters on fouling of 6061 aluminum alloy under dynamic conditions, *ES Materials & Manufacturing*, 2023, **21**, 893, doi: 10.30919/esmm893.
[29] V. Subbotina, O. Sobol, V. Belozerov, U. F. Al-Qawabeha, T. A. Tabaza, S. M. Al-Qawabah, V. Shnayder, A study of the electrolyte composition influence on the structure and properties of MAO coatings formed on AMg_6 alloy, *Eastern-European Journal of Enterprise Technologies*, 2020, **3**, 6-14, doi: 10.15587/1729-4061.2020.205474.
[30] V. Belozerov, O. Sobol, A. Mahatilova, V. Subbotina, T. A. Tabaza, U. F. Al-Qawabeha, S. M. Al-Qawabah, Effect of electrolysis regimes on the structure and properties of coatings on aluminum alloys formed by anode-cathode micro arc oxidation, *Eastern-European Journal of Enterprise Technologies*, 2018, **1**, 43-47, doi: 10.15587/1729-4061.2018.121744.
[31] V. Belozerov, O. Sobol, A. Mahatilova, V. Subbotina, T. A. Tabaza, U. F. Al-Qawabeha, S. M. Al-Qawabah, The influence of the conditions of microplasma processing (microarc oxidation in anode-cathode regime) of aluminum alloys on their phase composition, *Eastern-European Journal of Enterprise Technologies*, 2017, **5**, 52-57, doi: 10.15587/1729-4061.2017.112065.
[32] P. Zhang, Y. Zuo, G. Nie, The pore structure and properties of microarc oxidation films on 2024 aluminum alloy prepared in electrolytes with oxide nanoparticles, *Journal of Alloys and Compounds*, 2020, **816**, 152520, doi: 10.1016/j.jallcom.2019.152520.
[33] H. Sun, L. Li, Z. Wang, B. Liu, M. Wang, Y. Yu, Corrosion behaviors of microarc oxidation coating and anodic oxidation on 5083 aluminum alloy, *Journal of Chemistry*, 2020, **2020**, 6082812, doi: 10.1155/2020/6082812.
[34] H. Yu, Q. Dong, Y. Chen, C. Chen, Influence of silicon on growth mechanism of micro-arc oxidation coating on cast Al-Si alloy, *Royal Society Open Science*, 2018, **5**, 172428, doi: 10.1098/rsos.172428.
[35] L. Zhu, W. Zhang, T. Zhang, J. Qiu, J. Cao, F. Wang, Effect of the Cu content on the microstructure and corrosion behavior of PEO coatings on Al–*x*Cu alloys, *Journal of the Electrochemical Society*, 2018, **165**, 469-483, doi: 10.1149/2.0471809jes.
[36] W. Dai, C. Zhang, L. Zhao, C. Li, Effects of Cu content in Al-Cu alloys on microstructure, adhesive strength, and corrosion resistance of thick micro-arc oxidation coatings, *Materials Today Communications*, 2022, **33**, 104195, doi: 10.1016/j.mtcomm.2022.104195.
[37] W. Gao, J. Liu, J. Wei, Y. Yao, X. Ma, W. Yang, Enhanced properties of micro arc oxidation coating with Cu addition on TC4 alloy in marine environment, *Coatings*, 2021, **11**, 1168, doi: 10.3390/coatings11101168.
[38] T. Wei, F. Yan, J. Tian, Characterization and wear- and

corrosion-resistance of microarc oxidation ceramic coatings on aluminum alloy, *Journal of Alloys and Compounds*, 2005, **389**, 169-176, doi: 10.1016/j.jallcom.2004.05.084.
[39] F. Muhaffel, M. Baydogan, H. Cimenoglu, A study to enhance the mechanical durability of the MAO coating fabricated on the 7075 Al alloy for wear-related high temperature applications, *Surface and Coatings Technology*, 2021, **409**, 126843, doi: 10.1016/j.surfcoat.2021.126843.
[40] H. Siddiqui, M. R. Parra, M. S. Qureshi, M. M. Malik, F. Z. Haque, Studies of structural, optical, and electrical properties associated with defects in sodium-doped copper oxide (CuO/Na) nanostructures, *Journal of Materials Science*, 2018, **53**, 8826-8843, doi: 10.1007/s10853-018-2179-6.
[41] V. Rajkovic, D. Bozic, M. T. Jovanovic, Effects of copper and Al_2O_3 particles on characteristics of Cu–Al_2O_3 composites, *Materials & Design*, 2010, **31**, 1962-1970, doi: 10.1016/j.matdes.2009.10.037.
[42] A. M. Sadoun, M. M. Mohammed, E. M. Elsayed, A. F. Meselhy, O. A. El-Kady, Effect of nano Al_2O_3 coated Ag addition on the corrosion resistance and electrochemical behavior of Cu-Al_2O_3 nanocomposites, *Journal of Materials Research and Technology*, 2020, **9**, 4485-4493, doi: 10.1016/j.jmrt.2020.02.076.
[43] M. A. Ali Al-Mushaki, S. A. Al-Ariki, A. Alnehia, Effect of copper oxide (CuO) and vanadium oxide (V_2O_5) addition on the structural, optical and electrical properties of corundum (α-Al_2O_3), *Scientific Reports*, 2023, **13**, 16100, doi: 10.1038/s41598-023-43309-1.